A New Investigation on Tunnel Pool Fire Phenomenon Using CFD Technique

Babapoor, Aziz*+

Department of Chemical Engineering, University of Mohaghegh Ardabili, P.O. Box 179 Ardabil, I.R. IRAN

Bab, Vahid

Department of Chemical & Petroleum Engineering, Sharif University of Technology, Tehran, I.R. IRAN

Ahamdi Sabegh, Mehdi

Department of Chemistry, Ahar Branch, Islamic Azad University, Ahar, I.R. IRAN

ABSTRACT: *In this study, the amount of generated pool fire, as a result of the release of chemicals in the case of an accident in tunnels, was simulated and the results were compared to the experimental data. At first, various amounts of spatial resolution (R^*) were considered to compare the existing experimental data at different heights at the upstream, downstream and above the pool fire. The comparison studies showed that both numerical predictions and experimental measurements were, in general, comparable. Furthermore, FDS code was used to simulate the tunnel fire scenario for both cases of natural and forced ventilation. The grid using in the simulations is assessed by cells with the optimal spatial resolution and the influence of the ventilating systems on pool fire dynamic and its development was investigated. As a consequence, the temperature profile, O_2, CO_2, and visibility were compared in the two cases. These results showed that the ventilation system plays an important role in both fire development and heat removal by providing a safely evacuate rout in the tunnel.*

KEYWORDS: *Tunnel fire; CFD; FDS; Pool fire; Spatial resolution.*

INTRODUCTION

A number of accidents involving fatalities clearly shows that the risk associated with the transport of dangerous goods is significant and comparable with that of fixed plants [1]. Statistics also demonstrate that fire is the most frequent scenario among these accidents [2]. Several catastrophic fires had occurred in tunnels recently. Examples were the accidents in Mont-Blanc and Tauern in 1999, Gotthard in Switzerland in 2001, Dague in 2003, Frejus in Italy &France in 2005, Modane in France in 2005, Melbourne in 2007 and the recent one in Heysen Tunnels located in Adelaide Hills, 21 April 2009 [3]. Considering the disastrous consequence of tunnel fires and an unexpectedly large number of injuries and fatality, safety matters in tunnels are vital.

It is believed that a better understanding of the phenomenon of tunnel fire can effectively improve

***** *To whom correspondence should be addressed.*
+ E-mail: babapoor2006@yahoo.com ; babapoor@uma.ac.ir
1021-9986/2018/2/171-182 12/$/6.02

the safety condition. Accurate prediction of fire and smoke propagation in underground transportation is crucial in designing efficient fire protection systems. In general, fires are very complex in nature, such as turbulence, combustion radiation, combustible materials, fire location, space geometry, etc., which affect the fire and smoke propagation. Recently, using numerical simulation methods provide a better understanding of tunnel fires. Several models have been developed to simulate fire conditions in tunnels, ranging from simple analytical expressions to complex Computational Fluid Dynamics (CFD) codes. The analytical models have been used to calculate critical ventilation velocities, gas-phase velocities, and back-layering length; but their validity has occasionally been contested [4-8]. Zone models are more complex than the simple analytical expressions, addressing mass, momentum and heat transfer between different zones, which provide the values of temperatures in different spots, the concentration of components, mass flow rates, and velocities distribution [8-14].

Gorji and other researchers used computational techniques to solve simplified versions of the conservation equations. Over the past few years, with the dramatic advancement in computer processing power, modeling of fires has been shifted from the engineering application of correlation-based methods such as zone methods to filtered discrete solution equations by the CFD techniques [15-18].

The Fire Dynamics Simulator (FDS), developed by the National Institute of Standards and Technology (NIST), is receiving increasingly wide applications within the fire society. FDS is a CFD model of fire-driven fluid flow. The model numerically solves the Navier-Stokes equations, appropriate for low-speed, thermally-driven flow with an emphasis on smoke and heat transport from fires. The partial derivatives of the conservation equations of mass, momentum, and energy are approximated as finite differences, and the solution is updated in time on a three-dimensional, rectilinear grid. Thermal radiation is computed using a finite volume technique on the same grid as the flow solver. Lagrangian particles are used to simulate smoke movement, sprinkler discharge, and fuel sprays [19].

In this paper, the FDS code was used for the simulation of tunnel pool fires generated after the release of chemicals as a consequence of a hypothetical accident in a tunnel. In particular, a gasoline pool fire, consequent to a car crash and gasoline spilling, in a medium length tunnel was simulated. Predictions of the fire-induced temperatures, concentrations of pollutants and smoke, and of their evolution with or without a longitudinal ventilation system were calculated. Moreover, another parameter to study is appropriate mesh size used for the CFD simulating fire scenario in tunnels. Therefore, studies on the effects of mesh size were performed by launching several runs with different values of spatial resolution. For each run, the simulation results were compared with experimental data, and the required computing time was recorded.

THEORETICAL SECTION

Mathematical equations

Thermal-hydraulic models

The number of cells used in the grid, one of the most important numerical parameter in CFD, governs its numerical accuracy. The selection of mesh size for any CFD simulation significantly influences the predicted results for fire thermal characteristics. In pool fire modeling, finer meshes may provide better numerical solutions, but cause more computing costs. The necessary spatial resolution for a proper Large Eddy Simulation (LES) is expressed in terms of the characteristic diameter of a plume [20], which is defined by the following equation:

$$D^* = \left(\frac{Q}{\rho_\infty C_p T_\infty \sqrt{g}} \right)^{\frac{2}{5}} \quad (1)$$

The spatial resolution (R^*) of a numerical grid is defined as, the ratio of mesh size and pool fire diameter (D^*).

$$R^* = \frac{\Delta x}{D^*} \quad (2)$$

The necessary resolution suggested for single pool fire in most studies is between 1/5 and 1/10 [19, 21]. Other studies suggested a resolution of 1/20 to successfully predict the pool fire flame height [22].

FDS numerically solves a form of the *Navier-Stokes* equations appropriate for low speed, thermally-driven flow with an emphasis on smoke and heat transport from fires. The simplified relations for the conservation of mass, species, momentum, pressure equation and

the equation of state solved by FDS are presented below [14-17, 19-25]:

Conservation of mass:

$$\frac{\partial \rho}{\partial t} + u.\nabla \rho = -\rho \nabla u \tag{3}$$

Conservation of species:

$$\frac{\partial \rho Y_\alpha}{\partial t} + u.\nabla \rho Y_\alpha = -\rho Y_\alpha \nabla.u + \nabla.\rho D_\alpha \nabla Y_\alpha + \dot{m}_b''' \tag{4}$$

Conservation of momentum:

$$\frac{\partial u}{\partial t} + u \times \omega + \nabla H = -\frac{1}{\rho}((\rho - \rho_0)g + f_b + \nabla.\tau_{ij}) \tag{5}$$

Pressure equation:

$$\nabla^2 H = -\frac{\partial(\nabla.u)}{\partial t} - \nabla.F; F = u \times \omega - \frac{1}{\rho}((\rho - \rho_m)g - f_b - \nabla.\tau_{ij}) \tag{6}$$

Equation of state:

$$\bar{p}_m(z,t) = \rho R T \sum_\alpha {Y_\alpha}/{W_\alpha} \tag{7}$$

Since there is no analytical solution for the fully-turbulent *Navier-Stokes* equations, the solution of the above relations together requires the use of numerical methods, where the compartment is divided into a three-dimensional grid of small cubes.

Initial and boundary conditions

The tunnel inlet and outlet were set as the velocity boundary condition or pressure boundary condition. It is assumed that the outside surface of the tunnel lining is homothermal (temperature boundary) and the inner lining has one-dimensional heat conduction. As concrete is a poor conductor of heat, the actual lining thickness is generally large. The result obtained through the the heat-transfer calculation is appropriate to this and the temperature variation of the outside surface of the lining is small. The initial conditions and boundary conditions of the calculation simulation are as follows: initial relative pressure in the tunnel: 0 Pa; initial air density in the tunnel: 1.23 kg/m^3; initial temperature in the tunnel: 31°C; initial temperature of the tunnel lining concrete: 31°C; initial temperature of the fire source: 34°C; relative pressure of the tunnel outlet: 0 Pa ; tunnel inlet: constant velocity boundary condition; tunnel outlet: pressure outlet boundary condition; fire source: fluid source.

Turbulence model

One of the most important aspects of CFD modeling is the method of treating turbulence. CFD models can be divided into three major groups: a) Reynolds-Averaged Navier-Stokes (RANS) models, b) Large Eddy Simulation (LES) models and c) Direct Numerical Simulation (DNS) models. The core algorithm is an explicit predictor-corrector scheme, second order accurate in space and time. LES mode of FDS is used in this study. Turbulence is treated by means of the *Smagorinsky* form of LES [26] based on this analysis, the viscosity (μ) is modeled by the following equation:

$$\mu_{LES} = \rho(C_s \Delta)^2 \left(2.\bar{s}_{ij}.\bar{s}_{ij} - \frac{2}{3}(\nabla.\bar{u})^2 \right)^{\frac{1}{2}} \tag{8}$$

Combustion model

FDS uses the mixture fraction model as the default combustion model. The mixture fraction is a conserved scalar quantity. It is defined as the fraction of gas at a given point in the flow field that originated as fuel, as follows:

$$Z = \frac{s Y_F - (Y_O - Y_O^\infty)}{s Y_F^I + Y_O^\infty}; S = \frac{\nu_O W_O}{\nu_F W_F} \tag{9}$$

Starting with the most general form of the combustion reaction:

$$\nu_F Fuel + \nu_O O_2 \rightarrow \sum_i \nu_{p,i} product \tag{10}$$

The above equation implies that the mass consumption rates for fuel and oxidizer are related as follows:

$$\frac{\dot{m}_F'''}{\nu_F W_F} = \frac{\dot{m}_O'''}{\nu_O W_O} \tag{11}$$

The numbers ν_i are the stoichiometric coefficients for the overall combustion process that reacts fuel "*F*" with oxygen "*O*" to produce products "P".

The mixture fraction that represents the chemical reaction is solved by the governing equation:

$$\bar{\rho}\frac{DZ}{Dt} = \nabla.\bar{\rho}D_Z\nabla Z \quad (12)$$

Based on the assumption of ''infinitely fast reaction'', the oxygen and fuel cannot co-exist at any local point. This leads to the ''state relation'' between the oxygen mass fraction Y_O and the mixture fraction:

$$Y_O(Z) = \begin{cases} Y_O^{\infty}\left(1 - Z/Z_f\right) & Z < Z_f \\ 0 & Z > Z_f \end{cases} \quad (13)$$

Where Z_f defines a flame surface which is expressed as:

$$Z_f = \frac{Y_O^{\infty}}{sY_F^I + Y_O^{\infty}} \quad (14)$$

Radiation transport

Radiative heat transfer is included in the model by solving the Radiation Transport Equation (RTE) for a non-scattering grey gas, and in some limited cases, using a wideband model. The equation is solved using a technique similar to finite volume methods for convective transport; thus, the name given to it is the Finite Volume Method (FVM). In the case of a non-scattering gas, the RTE is expressed as [27, 28]:

$$s.\nabla I_\lambda(x,s) = \kappa(x,\lambda)[I_b(x) - I_\lambda(x,s)] \quad (15)$$

Prediction of smoke visibility

While CFD has become a proven tool for smoke modeling, the link between the numerical solution and the assessment of the environmental tenability is important and needs to be established. Among all the tenability criteria, such as temperature, radiant heat flux, and toxicity, the reduction in visibility due to smoke obscuration has been regarded as the most critical factor. An environment with low visibility would not only mean a much slower walking speed but also could incur psychological or hazardous consequences due to excessive heat exposure, intoxication or fall injuries. As the primary means of smoke control for underground transit stations is by ventilation, the smoke spread and hence tenability would be better understood by examining the visibility conditions. An appropriate method to evaluate visibility for CFD is, therefore, necessary [27]. Jin presented a number of models to predict visibility due to fire smoke, and the recent study has included in their mathematical correlation the effects of smoke adherence on exit signs. The most widely used visibility model, especially for CFD, is probably Jin's correlation, which states that the product of visibility, V, and the smoke extinction coefficient, C_s, is a constant, that is:

$$V \times C_s = K \quad (16)$$

where K is a constant and takes on different values for light emitting (K = 5 ~ 10) or reflecting signs (K = 2 ~ 4). The same formula has been implemented in the Fire Dynamic Simulator (FDS) [27, 28].

Verifying FDS Code

Full-scale simulations, as well as experimental data, were run using the FDS code in the prospect of using such code for realistic tunnel fire simulations. The tunnel at issue (Galleria "Colli Berici") is a two-tube road tunnel along the Northern Italy highway A4, between Milan and Venice, near the town of Vicenza. The tunnel is 550 m long, with a little slope (0.2%), with an arched cross section of 9.5 × 6.4 m. At the initial time, the ambient temperature was assumed to be 10 °C. The experimental data were available for a gasoline pool fire, about 1.2 m in diameter and 1 m high, located at the tunnel center. Experimental data had been collected in terms of gas temperature at five measurement stations (at the fire station (a): height 1.7 m, (b): height 5.2 m, at the station 20 m upstream the fire (a): height 5.2 m, (b): height 5.8 m, at the station 20 m downstream the fire: height 5.8 m). Results in terms of temperature profiles were available as the averaged temperature at different heights for each measurement station.

Numerical simulation for Galleria tunnel

Extended domain has been considered with dimensions of 750 m long, 9.5 m wide and 6.4 m height in a Cartesian coordinate system. The free pressure boundary conditions located 100 m away from each portal were applied on an extended domain boundary, where conditions were assumed to be ambient. The extended domain and boundaries of the tunnel are shown in Fig. 1.

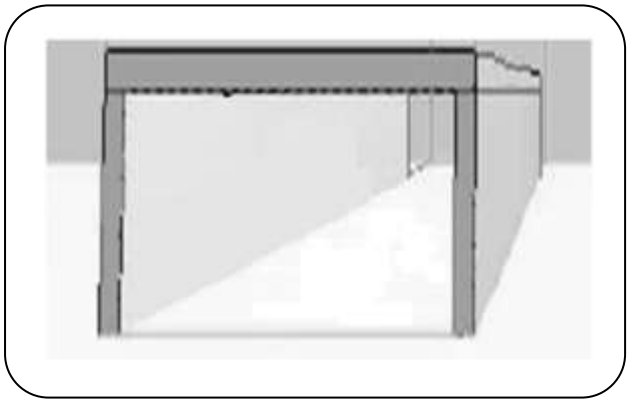

Fig. 1: Extended domain boundary of the tunnel.

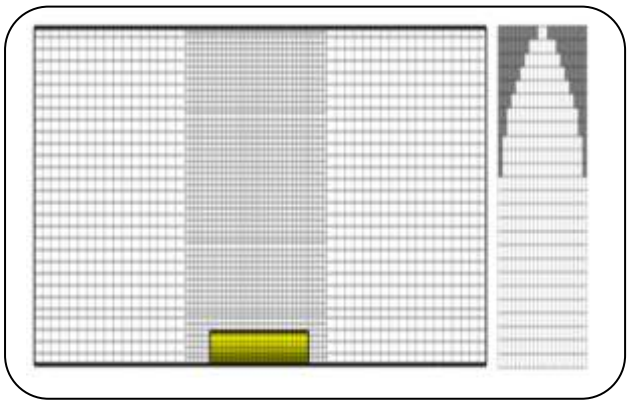

Fig. 2: Grid distribution in the tunnel.

The LES model for turbulence, the mixture fraction model for combustion and the finite volume method radiation model were selected in these simulations.

The curved cross-section of the tunnel was represented by stepwise grid approximation, because the FDS program adopted basically the rectangular grid system. In fact, these constructions of the stepwise grid change the smoke flow pattern near the curved surface. To lessen this impact on the smoke flow near the curved surface, the parameter SAWTOOTH was prescribed. Because grid size in LES code is directly concerned with filter width, grid spacing is very important to simulate fire driven flow. Different sizes of rectangular grids have been used for multi-mesh grids. This technique brings some flexibility to the grid generation and makes it possible to have a higher resolution in the desired areas. The grid using in simulations contains parallel rectangular cells so that the fire and the portals regions have finer cells than other regions of the tunnel. Fig. 2 shows the longitudinal grid distribution near fire source and cross-sectional grids for the tunnel used in the present study.

Mesh sensitivity and FDS code verifying

In order to investigate the influence of the size and resolution of the numerical grids, several Cartesian grids were assessed. The summary of mesh sizes, resolutions and required running time for these numerical grids were listed in Table 1.

The whole fire duration (30 min) was simulated. The results of tunnel fire simulations by using spatial resolutions which are represented in Table 1 were compared with the available experimental data. Fig. 3 through Fig. 5 show the comparison of experimental and predicted temperature profiles in the different height of the tunnel at the upstream, downstream and above the pool fire.

These figures, obviously show that none of the grids was able to reproduce good accuracy for the temperature profiles concurrently at all heights. In particular, the finer grid wasn't able to reproduce experimental data where the temperature gradients were fast and large (e.g. above the pool fire, Fig. 3-a) and, the other code parameters being equal, gave rise to a very large error in temperature profiles. On the other hand, the coarse grid, considering an average temperature on larger cells, underestimated the upper hot gas layers (the graphic for the fire section at height 5.2 m is reported, Fig. 3-b). Finally, the intermediate grid showed better fitting to the experimental data for the lower gas layer far from the fire (e.g. profiles at the measurement station at 20 m upwind are reported in Fig. 4). The simulation results globally showed that with the intermediate grid, the model effectively reproduced the experimental data reasonably well. Therefore, this sensitivity analysis on grid resolution from comparisons with experimental data led to the idea of using the intermediate grids as an optimized condition in the case study.

Case study

Siyahband is one of the several tunnels along the Haraz highway which is located between Tehran and Amol, in 47 Km from Rudehen. It is the main highway for the transportation of goods and passengers in northern Iran after Karaj-Chaloos Road, for example, each year over 4 million people use this road just in Nowrūz holiday [29]. The tunnel is a one tube tunnel (one-way) with about 328 m long, with an arched cross section of 10 ×7 m and it is equipped only with natural ventilation and has no fire mitigation systems. A gasoline pool fire in a tunnel was assumed as a scenario. A 6×6 m pool fire at the

Table 1: Summary mesh sizes / grid resolutions.

Mesh No.	$R^* = \frac{\Delta x}{D^*}$	Size of cells in fire station each axis (m)			Total number of cells	Running time (h)*
		IBAR	JBAR	KBAR		
1	0.67	0.79	0.79	0.8	28704	0.05
2	0.48	0.6	0.6	0.54	55104	0.12
3	0.34	0.5	0.3	0.4	67260	0.15
4	0.23	0.25	0.3	0.27	85792	0.5
5	0.14	0.17	0.16	0.18	288320	7
6	0.11	0.1	0.16	0.13	338572	13
7	0.09	0.075	0.14	0.11	493600	17
8	0.067	0.05	0.09	0.10	512700	23
9	0.05	0.039	0.042	0.088	690016	45

**: The simulation was run by a P4 computer with CPU 2.0 core 2 GHz and 1GB RAM, Main Domain: 750 ×9.5 × 6.4*

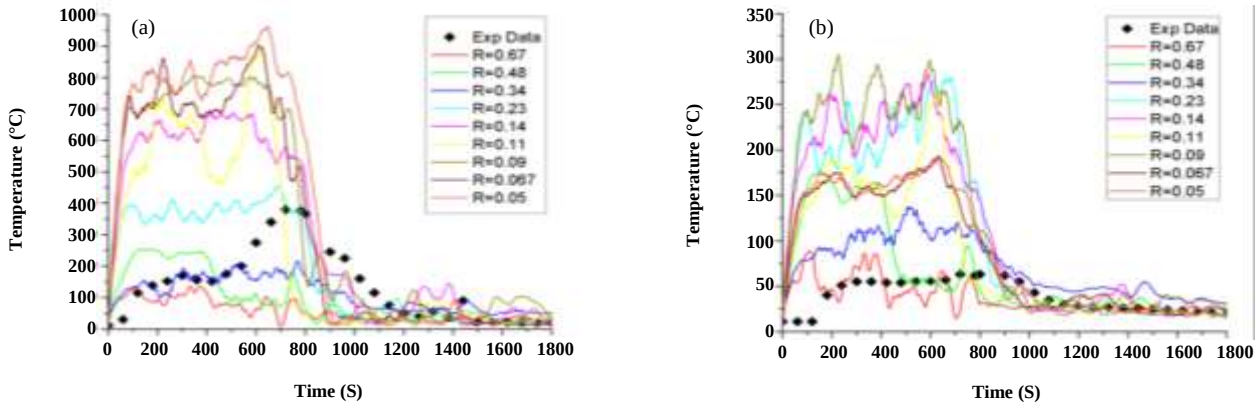

Fig. 3: Experimental and calculated temperature profiles at the fire station (a): height 1.7 m, (b): height 5.2 m.

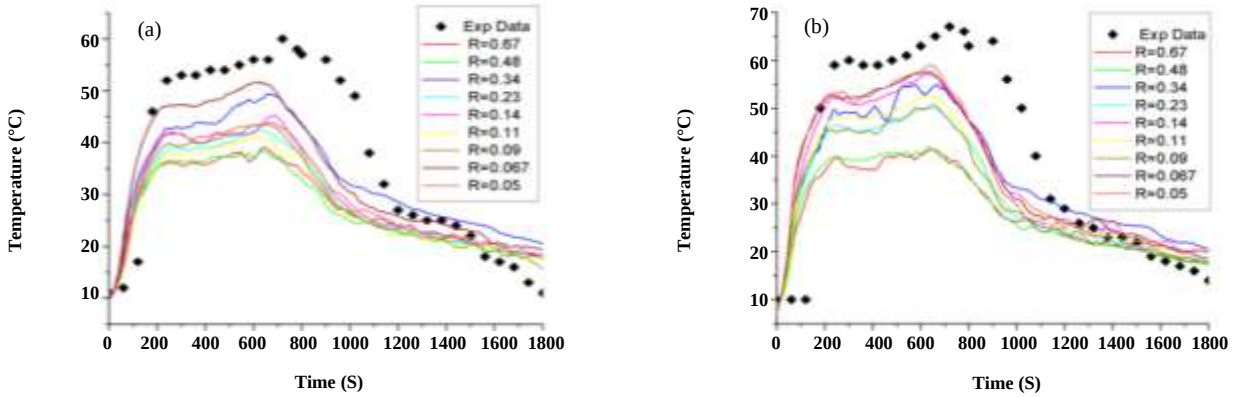

Fig. 4: Experimental and calculated temperature profiles at the station 20 m upstream the fire (a): height 5.2 m, (b): height 5.8 m.

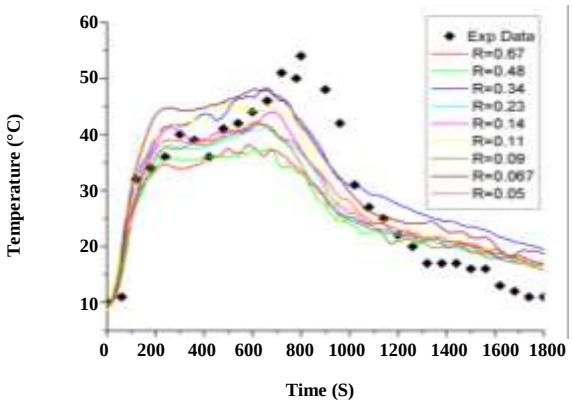

Fig. 5: Experimental and calculated temperature profiles at the station 20 m downstream the fire, height 5.8 m.

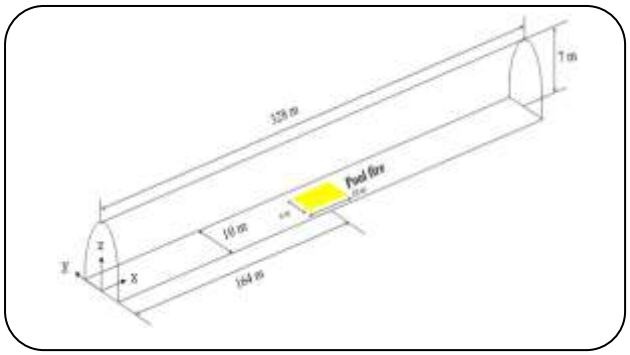

Fig. 6: The configuration and dimension of the Siyahband tunnel.

tunnel center was assumed to be subsequent to a medium release, lasting 10 min, from a hole in a road tanker. The tank (20 m^3, 6 m long, 2 m in diameter) was assumed to be stopped at a center of the tunnel. A 25 mm hole was supposed to form at the rear side of the tank, from which about 720 kg of gasoline spilled out in 10 min, generating an enlarging pool (10 mm in thickness) up to 6×6 m. The configuration and dimension of the model tunnel are shown in Fig. 6.

Numerical simulation of the Siyahband tunnel

The tunnel and boundary conditions were simulated with a grid consisting of about 238, 428 control volumes. A spatial refined grid was constructed around the fire source (with R^* = 0.3). To reproduce longitudinal ventilation, a uniform 0.13 m/s airflow was supplied at the $x = 0$ section. Free boundaries with the pressure equal to the static ambient pressure were assumed at the Portals. A gasoline pool, 6 m long, 6 m wide and 0.01 m high was placed at the middle of the tunnel.

RESULTS AND DISCUSSION

The survival aims for tunnel users must be to keep pollutants and toxic species concentrations below dangerous values (IDLH (Immediately Dangerous to Life or Health Concentrations) is 50000 ppm for CO_2), to guarantee a minimum O_2 concentration (17%vol) to allow breathing, to control smoke concentration such that illuminated signs should be discernible at 10 m and to provide survivable gas temperatures (i.e. not exceeding 60 °C) [30, 31].

In order to know whether people can safely escape the fire, the presumed location of pedestrians in the tunnel was evaluated by considering that the evacuation walking speed in a road tunnel in critical conditions can be assumed about 1.4 m/s, and taking also into account the time to perceive the risk and the time to react and leave the vehicle. If the walking speed is 1.4 m/s, the time for walking the maximum distance of 164 m in the tunnel is about 2 min; so the total time to run away can be assumed to be 3 min. The escape is assumed to start 60 s after ignition.

The normal breathing height inside the tunnel is between 1 and 3 m. The results of oxygen and carbon dioxide concentrations which are reported in Fig. 9-Fig. 12, are those calculated at 2.0 m from the tunnel floor. Simulation results are reported in Fig. 7 to Fig. 8 as space profiles of the gas temperature and in Fig. 9 and Fig. 10 as oxygen concentration, dioxide carbon concentration (Fig. 11 and Fig. 12) and visibility (Fig. 13 and Fig. 14) at different times (t = 36, 72, 108, 144 and 180 s) after the fire starts, during the early phase of the fire.

The results in Fig. 8 show how the longitudinal ventilation increases the temperature along the whole tunnel portion downstream the fire by carrying the combustion gases out, but at the same time, it keeps the temperature of upstream the fire low. In contrast, in the natural ventilation system, the calculated temperatures counters reported in Fig. 7, show that hot gases accumulate below the tunnel crown, spreading in both longitudinal directions, so the temperature in both sides increases dramatically. The results show that the maximum temperature for natural ventilation is approximately 350°C higher than the maximum temperature in the forced ventilation system.

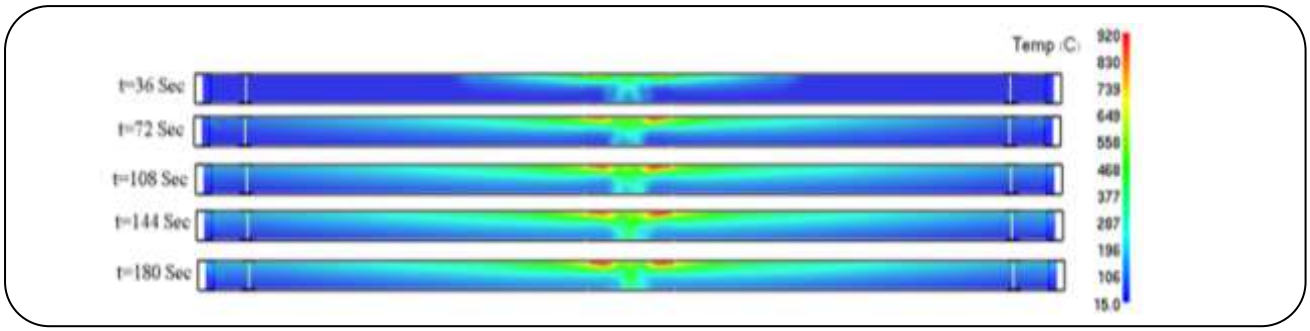

Fig. 7: Time evolution (0-3 min) of temperature counters in centerline, natural ventilation.

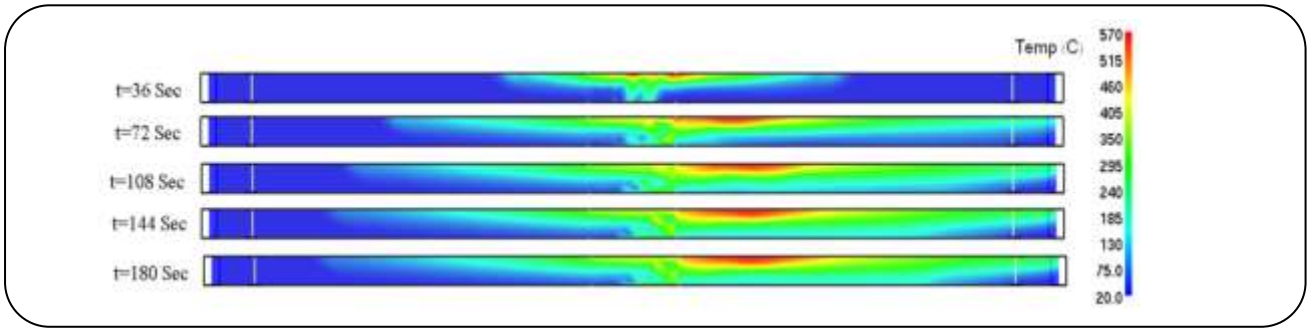

Fig. 8: Time evolution (0-3 min) of temperature counters in centerline, forced ventilation system.

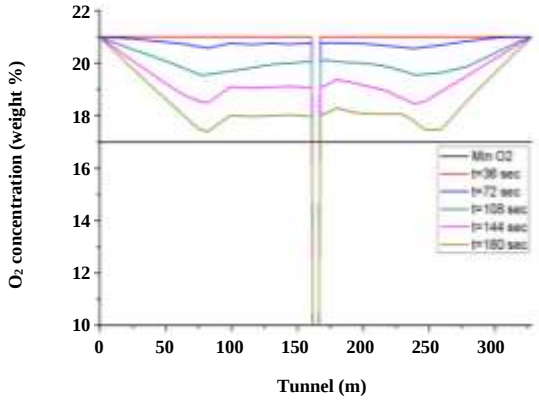

Fig. 9: Time evolution (0-3 min) of oxygen concentration profiles, tunnel centerline, and height=2.0 m, natural ventilation.

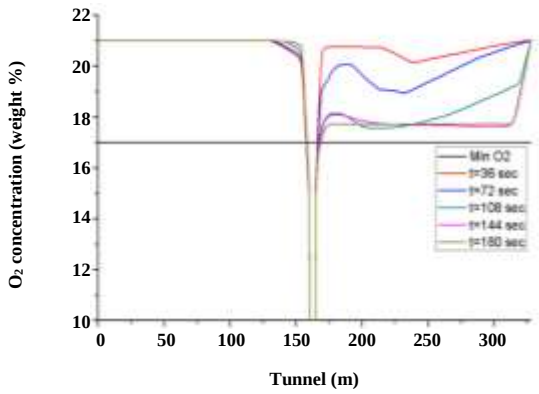

Fig. 10: Time evolution (0-3 min) of oxygen concentration profiles, tunnel centerline, and height=2.0 m, forced ventilation System.

However, in natural ventilation, oxygen and carbon dioxide concentrations remain within safety ranges (Fig. 9 and Fig. 11), while visibility, at t=120 s is already below than the minimum recommended value (Fig. 13). As a result, either because of the relatively high temperature or because of the blurred vision, people would not be able to reach the tunnel exit. Indeed, the worsened conditions further decrease the velocity of people at which they can escape.

O_2 and CO_2 concentrations and visibility with the longitudinal ventilation system are reported in Fig. 10, Fig. 12 and Fig. 14. From all the figures, it is evident that upstream the fire, the conditions remain safe for evacuation and rescue during the fire evolution. The comparison between the results of the simulation in the presence and absence of forced ventilation clearly shows that there are marked differences of the safety level of pedestrians escaping from the fire. The difference is due

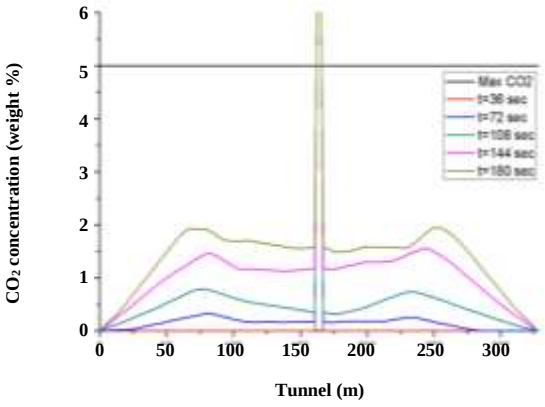

Fig. 11: Time evolution (0-3 min) of dioxide carbon concentration profiles, tunnel centerline, and height=2.0 m, natural ventilation.

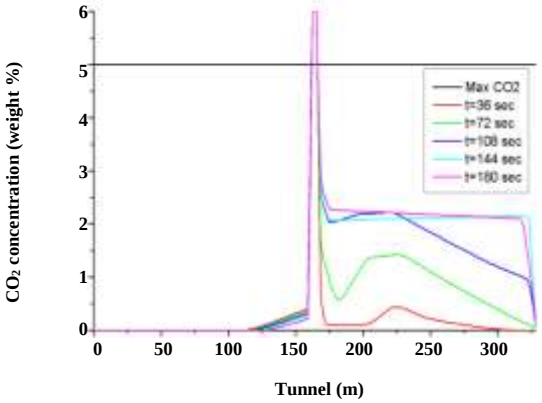

Fig. 12: Time evolution (0-3 min) of dioxide carbon concentration profiles, tunnel centerline, and height=2.0 m, forced ventilation system.

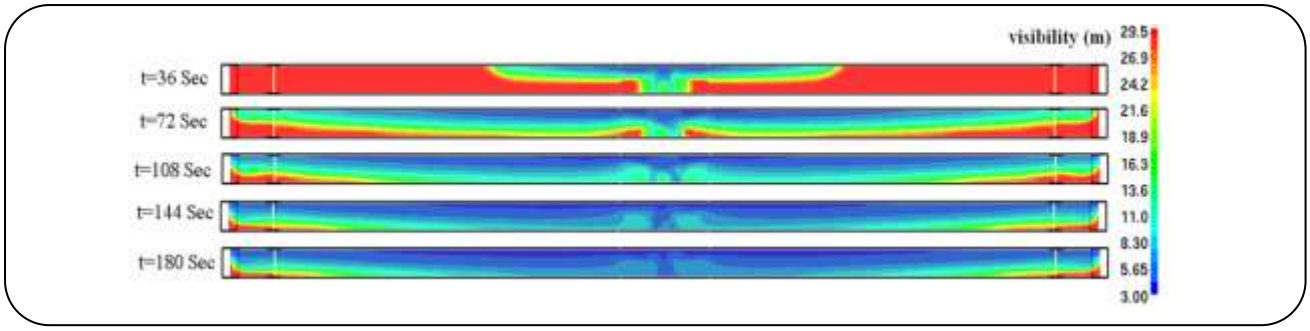

Fig. 13: Time evolution (0-3 min) of visibility counters in centerline, natural ventilation.

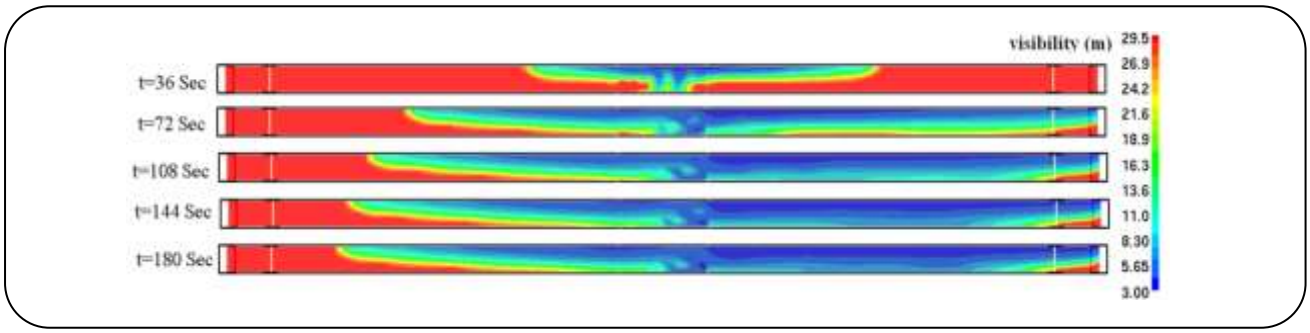

Fig. 14: Time evolution (0-3 min) of visibility counters in the centerline, forced ventilation system.

to the longitudinal ventilation system that is able to force the smoke and hot gases in the direction of the unoccupied tunnel so providing a clear and safe environment behind the fire for evacuation and rescue. Compared to the natural ventilation, the forced ventilation has a further positive effect: it strongly limits tunnel structural damages, because very high gas temperatures occur only in a small region and for a short time. In light of such results, it could be useful to reconsider the limiting length above which a tunnel along the road and railway routes used for chemicals or dangerous goods transportation should be equipped with proper ventilation systems. Indeed, a forced ventilation system can make the difference between the life and the dead of at least part of the involved people**.**

Carbon monoxide inhibits the ability of blood to carry oxygen to vital organs. Inhaled, *CO* will combine with oxygen carried by hemoglobin in the blood and will form

Table 2: Health effects of CO.

Exposure(h)	CO Concentration (ppm)		
	Perceptible	Sickness	Deadly
0.5	600	1000	2000
1	200	600	1600
2	100	300	1000
4	50	150	400
6	25	120	200
8	25	100	150

carboxyhemoglobin (COHb) which inhibits oxygen transportation. But considering the fact that high concentrations carbon monoxide (about 12000 ppm) is fatal after 1-3 minutes, while and lower concentration such as 1600 ppm is deadly after one hour, and also taking the assumption of complete combustion into consideration, the amount of CO produced by fire does not affect the calculations considerably. Health effects of carbon monoxide were presented at Table 2.

CONCLUSIONS

The simulations for the hypothesized accident by CFD technique allowed carrying a deep study on usefulness and effectiveness ventilation systems. Natural ventilation was not sufficient to ensure safe conditions for escape and rescue operations. Consequences on safety could be serious because of the rapid increase of temperature and smoke concentration, strongly compromising the possibility for people to safely evacuate the tunnel. The results suggest that it could be opportune to reconsider the limiting length above which a tunnel along the road and railway routes used for chemicals or dangerous goods transportation should be equipped with proper ventilation systems. In addition, the paper is investigated the effect of mesh size in CFD ability to simulate the characteristics involved in the tunnel pool fires. Based on the sensitivity study of different mesh sizes, all the grid resolutions generally reproduce good prediction of tunnel behavior, but the predicted temperature profile have more consistency with experimental data when intermediate mesh ($0.2< R^*<0.4$) was used in numerical modeling of tunnel pool fire scenario.

Nomenclature

C_s	Smagorinsky's constant
C_p	Specific heat capacity, J/kg.K
D	Diffusion coefficient, m^2/s
D*	Characteristic diameter, m
g	Gravitational acceleration, m^2/s
s	Unit vector in direction of radiation intensity
I	Total radiation intensity
I_b	Radiation blackbody intensity
$\dot{m}'''$	Mass consumption rate per unit volume, kg/m^3 s
P	Pressure, N/m^2
T	Temperature, K
u=(u,v, *w*)	Velocity vector, m/s
R	Ideal gas constant, 8.314 J/mol K
R^*	Normalized mesh size
t	Time, s
P	Pressure, N/m^2
P_0	Background pressure, N/m^2
Q	Heat source, W/m^3
$\bar{p}_m$	Background pressure of m^{th} pressure zone
H	Total pressure divided by the density
f_b	External force vector (excluding gravity)
W	Molecular weight, kg
x	Coordinate, m
Y_F^I	Fuel mass fraction in the fuel stream
Y_o^∞	Ambient value of fuel mass fraction
Z	Mixture fraction
Y	Mass fraction

Greek symbol

Δ	Mesh size, m
∇	Gradient
μ	Viscosity, kg/m s
ρ	Density, kg/m^3
υ	Stoichiometric coefficient
κ	Absorption coefficient
τ	Shear force, N/m^2
Γ	Thermal conductivity, W/m K
λ	Radiation intensity at a wavelength

Subscript

F	Fuel
i, j, k	Tensor index
l	lth species
α	Gas species
O	Oxygen
P	Product
∞	Ambient parameter

Superscript

–	Averaging parameter

Received: Jun. 1, 2016; Accepted: Jan. 15, 2018

REFERENCES

[1] Khan F.I., Abbasi S.A., Major Accidents in the Process Industries and an Analysis of Their Causes and Consequences, *J. Loss Prev. Process Ind.*, **12**(5): 361-374 (1999).

[2] *Vilchez J.A.*, Sevilla S., Montiel H., Casal J., Historical Analysis of Accidents in Chemical Plants and in the Transportation of Hazardous Materials, *J. Loss Prev. Process Ind.*, **8**(2): 87–96 (1995).

[3] Charters D.A., Gray W.A., McIntosh. A.C., A Computer Model to Assess Fire Hazards in Tunnels (FASIT), *Fire Technol.*, **30**(1): 134-154 (1994).

[4] Grant G.B., Jagger S.F., Lea C.J., Fires in tunnels, *Philos. Trans. R. Soc. London, Ser. A*, **356**(1748): 2873-2906 (1998).

[5] Megret O., Vauquelin O., Model to Evaluate Tunnel Fire Characteristics, *Fire Saf. J.*, **34**(4): 393-401 (2000).

[6] Jafari A., Shahmohammadi A., Mousavi S.M., CFD Investigation of Gravitational Sedimentation Effect on Heat Transfer of a Nano-Ferrofluid, *Iran. J. Chem. Chem. Eng.(IJCCE)*, **34**(1): 87-96 (2015).

[7] Carvel R.O., Beard A.N., Jowitt P.W., Drysdale D.D., The Influence of Tunnel Geometry and Ventilation on the Heat Release Rate of a Fire, *Fire Technol.*, **40**: 5-26 (2004).

[8] Ingason H., Lönnermark A., Heat Release Rates from Heavy Goods Vehicle Trailers in Tunnels, *Fire Saf. J.*, **40**: 646-668 (2005).

[9] Mouangue R., Onguene P.M., Zaida J.T., Ekobena H.P., Numerical Investigation of Critical Velocity in Reduced Scale Tunnel Fire with Constant Heat Release Rate, *J. Combust.*, **2017**: 1-12 (2017). https://doi.org/10.1155/2017/7125237.

[10] Lai H., Wang S., Yongli Xie Y., Study on the Fire Damage Characteristics of the New Qidaoliang Highway Tunnel: Field Investigation with Computational Fluid Dynamics (CFD) Back Analysis, *Int. J. Environ. Res. Public Health*, **13:** 1-16 (2016). DOI:10.3390/ijerph13101014.

[11] Muhasilovic M., Duhovnik J., CFD-Based Investigation of the Response of Mechanical Ventilation in the Case of Tunnel-Fire, *J. Mech. Eng.*, **58**(3): 183-190 (2012).

[12] Hwang C.C., Wargo J.D., Experimental Study of Thermally Generated Reverse Stratified Layers in a Fire Tunnel, *Combust. Flame*, **66**(2): 171-180 (1986).

[13] Daish N.C., Linden P.F., "Interim Validation of Tunnel Fire Consequence Models: Comparison Between the Phase 1,Trails Data and the CREC/HSE Near-Fire Model", Cambridge Environmental Research Consultants, **FM88/92/6** (1994).

[14] Nazghelichi T., Jafari A., Kianmehr M.H., Aghbashlo M., CFD Simulation and Optimization of Factors Affecting the Performance of a Fluidized Bed Dryer, *Iran. J. Chem. Chem. Eng.(IJCCE)*, **32**(4): 81-92 (2013).

[15] Gorji M., Bozorgmehry Boozarjomehry R., Kazemeini M., CFD Modeling of Gas-Liquid Hydrodynamics in a Stirred Tank Reactor, *Iran. J. Chem. Chem. Eng.(IJCCE)*, **26**(2): 85-96 (2007).

[16] Kashef A., Benichou V., Lougheed G., Debs A., "Application of CFD Techniques for Modelling Fire Tests in Road Tunnels", *12th Annual Conference of the Computational Fluid Dynamics Society of Canada*, Ottawa, Ontario, 288-289 (2004).

[17] Shabanian S.R, Rahimi M., Khoshhal A., Abdulaziz Alsairafi A., CFD Study on Hydrogen-Air Premixed Combustion in a Micro Scale Chamber, *Iran. J. Chem. Chem. Eng.(IJCCE)*, **29**(4): 161-172 (2010).

[18] Yucel N., Berberoglu M.I., Karaaslan S., Dinler N., Experimental and Numerical Simulation of Fire in a Scaled Underground Station, *World Acad. Sci. Eng. Technol*., **40**: 309-314 (2008).

[19] McGrattan K., "Fire Dynamics Simulator (Version 4), Technical Reference Guide", NIST Special Publication 1018, National Institute of Standards and Technology, Gaithersburg, Maryland, (2004).

[20] Dreisbach J., McGrattan K., "Verification and Validation of Selected Fire Models for Nuclear Power Plant Applications", Volume 7: "Fire Dynamics Simulator (FDS)", NUREG-**1824** Final Report, U.S. Nuclear Regulatory Commission, Office of Nuclear Regulatory Research, May (2007).

[21] Wang H.Y., Coutin M., Most J.M., Large Eddy Simulation of Buoyancy Driven Fire Propagation Behind a Pyrolysis Zone Along a Vertical Wall, *Fire Saf. J.*, **37**(3): 259-585 (2002).

[22] Ma T.G., Quintiere J.G., Numerical Simulation of Axi-Symmetric Fire Plumes: Accuracy and Limitations, *Fire Saf. J.*, **38:** 467-492 (2003).

[23] Aghaaliakbari B., Jafari Jaid A., Zeinali M.A.A., Computational Simulation of Ablation Phenomena in Glass-filled Phenolic Composites, *Iran. J. Chem. Chem. Eng.(IJCCE)*, **34**(1): 97-106 (2015).

[24] Zakeri A., Pazouki M., Vossoughi M., Use of Response Surface Methodology Analysis for Xanthan Biopolymer Production by Xanthomonas campestris: Focus on Agitation Rate, Carbon Source, and Temperature, *Iran. J. Chem. Chem. Eng.(IJCCE)*, **36**(1): 173-183 (2017).

[25] Yousefpour M., Modelling of Adsorption of Zinc and Silver Ions on Analcime and Modified Analcime Zeolites Using Central Composite Design, *Iran. J. Chem. Chem. Eng. (IJCCE)*,**36**(4): 81-89 (2017).

[26] Smagorinsky J., General Circulation Experiments with the Primitive Equations, I-The Basic Experiment, *Mon. Weather Rev.*, **91**(3): 99–164 (1963).

[27] Kang K., Prediction of Smoke Visibility During an Underground Rail Station Fire, *Int. Assoc. Fire Saf. Sci.*, **1:** 1-13 (2007).

[28] Jin T., Yamada T., Irritating Effects of Fire Smoke on Visibility, *Fire Sci. Technol.*, **5**(1): 79-90 (1985).

[29] http://en.wikipedia.org/wiki/Road_77_(Iran).

[30] NIOSH-CDC, Documentation for Immediately Dangerous to Life or Health Concentrations (IDLH), Available from: http://www.cdc.gov/niosh/idlh/intridl4.html.

[31] Rom W., "Environmental and Occupational Medicine", 4th ed, Lippincott Williams & Wilkins, Philadelphia (2007).